Antiferromagnetic Structure of CrN†

L. M. CORLISS, N. ELLIOTT, AND J. M. HASTINGS
Chemistry Department, Brookhaven National Laboratory, Upton, New York
(Received August 3, 1959)

Chromium nitride, crystallizing with the rock salt structure, has been found to be antiferromagnetic with a Néel point of 0°C. The magnetic ordering scheme, as determined by neutron diffraction, is that of the fourth kind, with moments arranged in double ferromagnetic sheets which alternate along a line parallel to a face-diagonal. The structure is orthorhombic below the transition and the space group *Pnma* has been tentatively assigned. The atomic displacements accompanying the distortion have been partially determined from the diffraction data and are discussed in relation to the magnetic structure. A value of 2.4 μ_B has been assigned to the Cr moment; the moment direction is parallel to the *b* axis of the orthorhombic cell (face-diagonal of the cube).

INTRODUCTION

CONSIDERABLE attention has been directed in recent years toward the determination of spin arrangements in antiferromagnetic iron-group compounds crystallizing with the NaCl structure. Neutron diffraction studies[1] of a number of oxides, sulfides, and selenides have shown that in all these compounds the antiferromagnetic structure is characterized by an arrangement in which next-nearest neighbor spins are oriented antiparallel to one another. Atoms separated by unit translations parallel to the axes of the chemical unit cell thus have their moments oppositely directed below the Néel point.

The magnetic structure has been further characterized as consisting of a sequence of ferromagnetically aligned (111) sheets which alternate in sign. This description is consistent with powder diffraction data but requires the assumption that spins are all parallel or antiparallel to a single direction in the crystal. It has been pointed out[2] that this model is not unique and that it is possible to choose a number of noncollinear spin arrangements which are consistent with the powder data. It should be noted in this connection that the conclusion that next-nearest neighbors are antiparallel can be unambiguously deduced from the diffraction extinctions and is independent of the assumption of collinearity.

This antiparallel coupling is stabilized by a superexchange interaction proceeding via the anion located midway between each pair of magnetic ions. In fact, Anderson[3] has concluded that if the exchange utilizes the *p* electrons of the anion it would result in strong antiferromagnetic coupling between the cations symmetrically located on either side of the anion. Thus the linear coupling scheme $M\uparrow-X-M\downarrow$ found in rock salt structures would appear to depend upon the correlation of anion *p* electrons in the same state and to derive its directionality from the shape of the *p*-wave function.

The rock salt compounds hitherto investigated by means of neutron diffraction are all largely ionic in character. It would be of interest, from the point of view of the superexchange mechanism, to examine compounds in which the bonding is appreciably more covalent and in which, at the same time, the rock salt structure is retained. In this paper we consider the case of CrN, a nonionic, interstitial compound, which we have found to be antiferromagnetic. In contrast to most oxides and sulfides, interstitial compounds of this type are characterized by exceedingly high melting-points, suggesting that very strong metal to nonmetal bonds are present. Pauling[4] has suggested that in compounds involving first-row elements, where the maximum number of covalent bonds is four, these bonds may resonate among the six positions available at an octahedral site. More recently, the interstitial compounds have been extensively discussed by Rundle,[5] who proposes a new bonding scheme to explain the many striking physical properties of these compounds. We will return to a consideration of Rundle's theory after the presentation of experimental results since the antiferromagnetic structure of CrN may be correlated in an interesting way with his proposed general model.

Preparation and Magnetic Measurements

Eimer and Amend "carbon free" chromium was finely ground and sieved through a No. 200 sieve. Its magnetic susceptibility was measured after passage through a magnetic separator, and found to agree with accepted published measurements.

A sample of this chromium was nitrided at 1100°C with NH_3 that was dried over sodium and passed

† Research performed under the auspices of the U. S. Atomic Energy Commission.

[1] C. G. Shull, W. A. Strauser, and E. O. Wollan, Phys. Rev. **83**, 333 (1951); L. M. Corliss, N. Elliott, and J. Hastings, Phys. Rev. **104**, 924 (1956); W. L. Roth, Phys. Rev. **110**, 1333 (1958).

[2] W. L. Roth, Phys. Rev. **111**, 772 (1958); A. L. Loeb and J. B. Goodenough, *Conference on Magnetism and Magnetic Materials*, pp. 55–68; *Boston, 1956* (American Institute of Electrical Engineers, New York, 1957), Spec. Publ. T91, A. L. Loeb, Acta Cryst. **11**, 469 (1958); F. Keffer and W. O'Sullivan, Phys. Rev. **108**, 637 (1957).

[3] P. W. Anderson, Phys. Rev. **79**, 350 (1950).

[4] L. Pauling, *The Nature of the Chemical Bond* (Cornell University Press, Ithaca, 1948).

[5] R. E. Rundle, Acta Cryst. **1**, 180 (1948).

TABLE I. Molar susceptibility of CrN.

Temperature °K	325	297	282	273	258	225	77
$\chi_M(\times 10^6)$	745	763	800	755	620	505	450

through a fine sintered glass filter. Successive grindings and nitridings were necessary to yield a specimen that was substantially free of the lower nitride, Cr_2N.

Several samples were prepared in the above manner and all showed a slight ferromagnetic impurity which we have tentatively ascribed to Cr_2N. In order to measure the susceptibility a procedure involving an extrapolation to infinite field was used. The measurements were made by an induction method using a cylindrical sample placed in a uniform field. A current was then passed through a coil wound around the sample and adjusted to restore the uniform field. The current is then a measure of the magnetization. The apparatus was calibrated both on an absolute basis from the dimensions of the coil and on a relative basis using ferrous ammonium sulfate. Table I lists the susceptibility as a function of temperature for CrN determined in this manner. A plot of the data given in Fig. 1 shows a rather sharp antiferromagnetic transition at about 0°C.

DIFFRACTION DATA

Neutron powder diffraction patterns were obtained at room temperature, liquid nitrogen and liquid helium temperatures. Typical patterns, taken at a wavelength of 1.064 A, are shown in Fig. 2. The room temperature data indexes as a cubic rock salt structure having an a_0 equal to 4.13 A, and shows a slight Cr_2N impurity. The liquid nitrogen data shows a well developed superstructure and requires a doubling of the original unit cell in two directions in order to index the new lines. There is practically no difference between the 77°K and the 4.2°K patterns. The pseudocubic indices shown at the bottom of the 77°K pattern in Fig. 2 are for a unit cell which, for the sake of convenience, has been doubled in all three directions. The fact that the unit cell must be doubled in two directions in order to index the peaks implies that the ordering scheme of the magnetic moments is of the fourth kind, shown in Fig. 3. In this kind of ordering, assuming collinear spins, the twelve nearest neighbor magnetic moments are half parallel and half antiparallel to the central moment; while of the six next-nearest neighbors, four are antiparallel and two parallel. The nearest neighbor distribution is thus the same as in ordering of the second kind which is the only type of magnetic ordering heretofore observed in rock salt structures. The six next-nearest neighbor moments however are all antiparallel in ordering of the second kind as compared with only four in ordering of the fourth kind. In the latter kind there are two possible ways in which the four interpenetrating substructures may be combined leading to either alternating double ferromagnetic sheets in one direction [110], (a) of Fig. 3; or alternating single ferromagnetic sheets interleaved with mixed sheets propagated in two direction at right angles to each other [110 and $1\bar{1}0$], (b), of Fig. 3. It should be noted that the product of the structure factor and multiplicity, jF^2, for the two possible models are identical so that they are indistinguishable on the basis of powder intensity measurements. However, as will be shown later, this ambiguity can be eliminated on the basis of the superstructure peak positions. All attempts at varying both the spin direction and magnetic form factor in order to obtain suitable agreement between calculated and observed integrated intensities for the magnetic peaks based on this model failed. Table II lists the calculated intensities for several of the simple spin directions tried, together with the [310] direction which gave the best fit. Even for this last direction the disagreement between calculated and observed intensities is considerably greater than the experimental error and forces one to conclude that the model is unsatisfactory in detail. All of the calculated intensities listed in the table are based upon a Mn^{++} form factor. The nature of the discrepancies is such, however, as to rule out the possibility of modifying the Mn^{++} form factor in a reasonable manner and thereby obtaining a satisfactory fit.

A careful examination of the neutron diffraction patterns (Fig. 2) shows that below the Néel point the (111) nuclear peak of the original unit cell has decreased by about a factor of two. Simultaneously the (111) peak from the aluminum cryostat and cell has increased in intensity and half-width indicating the superposition of some extra scattering from the sample. This together with the appearance below the Néel point of a small peak around 33° in 2θ, which could not be

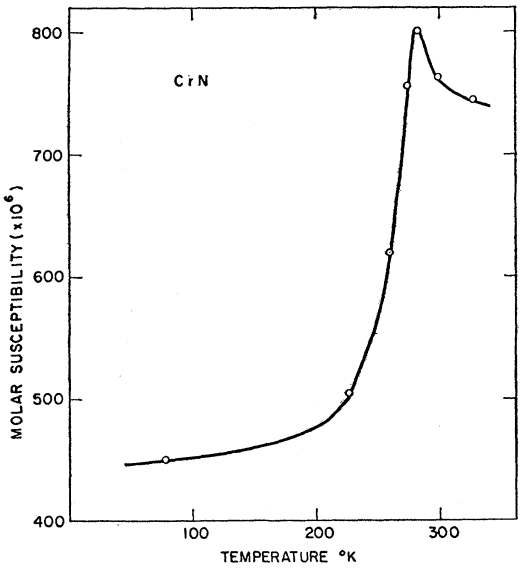

FIG. 1. Molar susceptibility of CrN as a function of temperature.

indexed by the simple magnetic model, led us to investigate the possibility of a crystal distortion accompanying the transition. X-ray diffraction measurements above and below the Néel point are shown in Fig. 4. It is clear that a relatively large distortion has set in below the magnetic transition. The low-temperature x-ray pattern can be indexed using an orthorhombic unit cell which is related to the double cubic

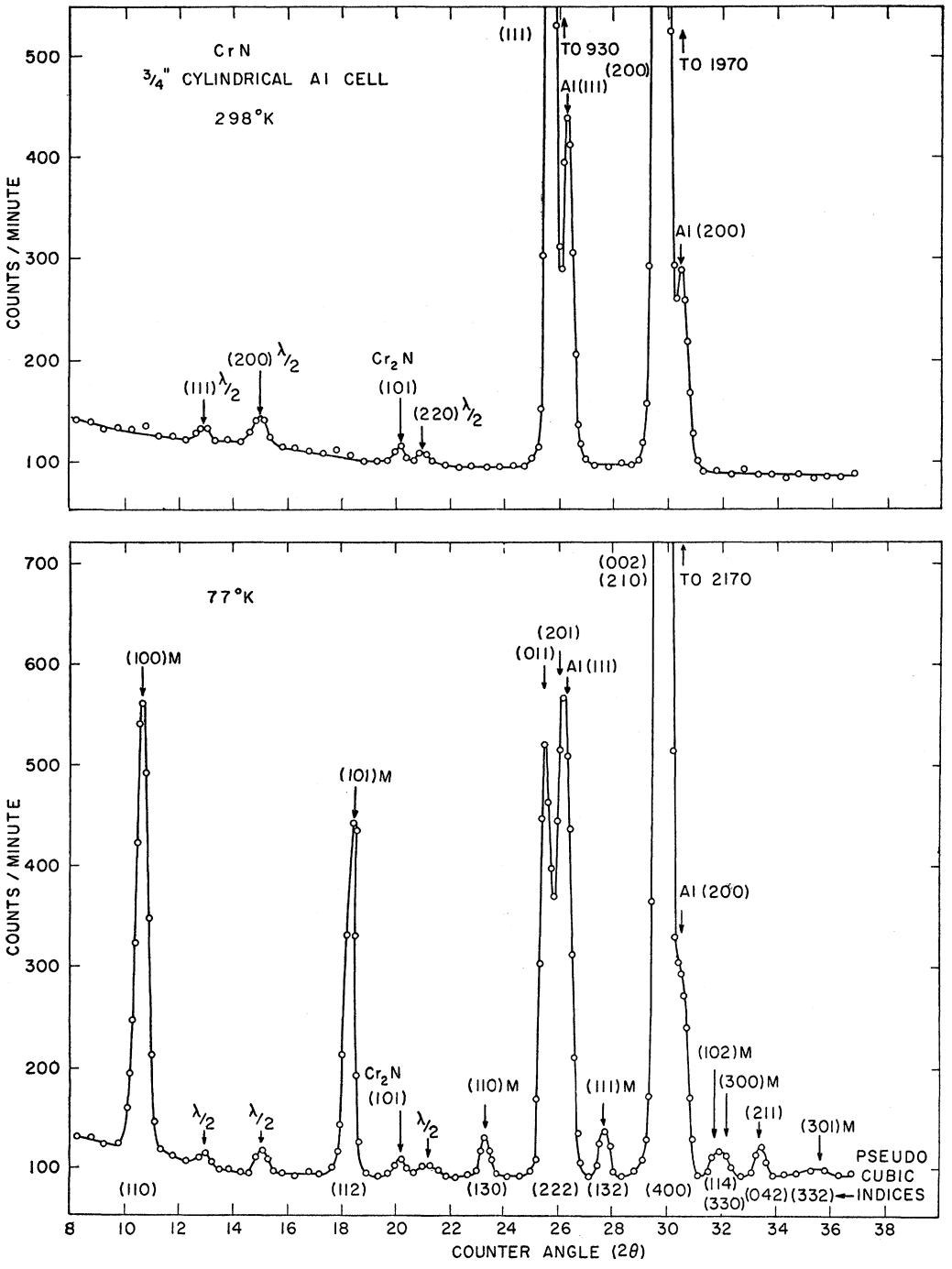

FIG. 2. Neutron diffraction patterns of CrN taken at 298°K and at 77°K. Reflections indicated by Al(*hkl*) are produced by the aluminum components of the cryostat and sample holder; second order wavelength contributions are designated by λ/2. The room temperature pattern is indexed on a cubic cell whereas the low-temperature pattern is referred to the orthorhombic cell shown in Fig. 5. Magnetic superstructure lines are denoted by the letter *M*.

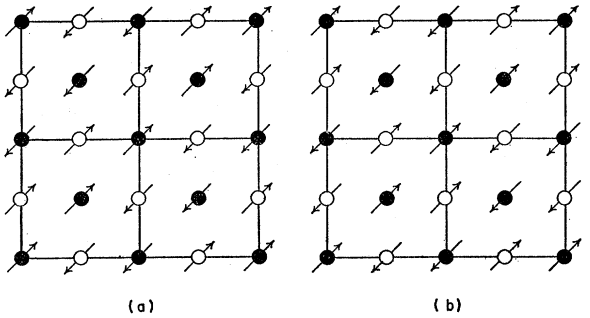

FIG. 3. Two possible arrangements of magnetic moments for ordering of the fourth kind. Solid circles refer to atoms at the $z=0$ level and open circles to atoms at $z=\frac{1}{2}$. In (a) the moments are arranged in alternating pairs of ferromagnetic sheets parallel to a single face diagonal whereas in (b) ferromagnetic sheets of opposite sign are interleaved with neutral sheets and the structure is propagated parallel to two face diagonals.

cell as shown in Fig. 5. A comparison between calculated and observed line positions for the orthorhombic structure is given in Table III. This distortion explains the decrease in intensity of the original (111) nuclear peak in the neutron diffraction pattern below the Néel point since it splits into the (011) and (201) peaks of the orthorhombic structure and the latter nearly coincides with the Al (111) peak. The small peak in the neighborhood of 33° in counter angle previously mentioned can also be accounted for on the basis of this distortion as will be shown subsequently. Incidentally, it is this distortion which enables one to choose between the two alternative forms of ordering of the fourth kind. Model (a) of Fig. 3, as has been mentioned previously, has a unique direction for the ferromagnetic sheets while model (b) propagates ferromagnetic sheets in two directions. As a consequence of the orthorhombic distortion, the two directions of propagation of model (*g*) become inequivalent, resulting in a splitting of the magnetic lines. Table IV lists the observed and calculated peak positions for the two models and establishes the essential correctness of model (*a*).

TABLE II. Comparison of calculated and observed magnetic intensities in pseudocubic approximation.

hkl (pseudocubic indices)	Calculated intensities Spin direction [100]	[110]	[1$\bar{1}$1]	[310]		Observed intensity
110	838	838	838	838	↔	838
112	685	411	685	479		560
130	187	38	488	75		60
132	254	84	479	127		86
114+330	131	83	131	96		95

SPACE GROUP CONSIDERATIONS

It is perhaps not too surprising, in view of the distortion which sets in below the Néel point, that magnetic intensities calculated for a cubic structure fail to accord well with the observed intensities. The reduction in symmetry may be accompanied by a motion of atoms away from the special positions corresponding to the NaCl structure, thus significantly modifying the computed superstructure intensities. In principle, all the information required to obtain a fit with the experimental results is contained in the magnetic space group, which provides not only a set of allowed positions for all atoms, but also a set of allowed spin arrangements and orientations with respect to cell axes. The application of space group methods to the determination of magnetic structures has been

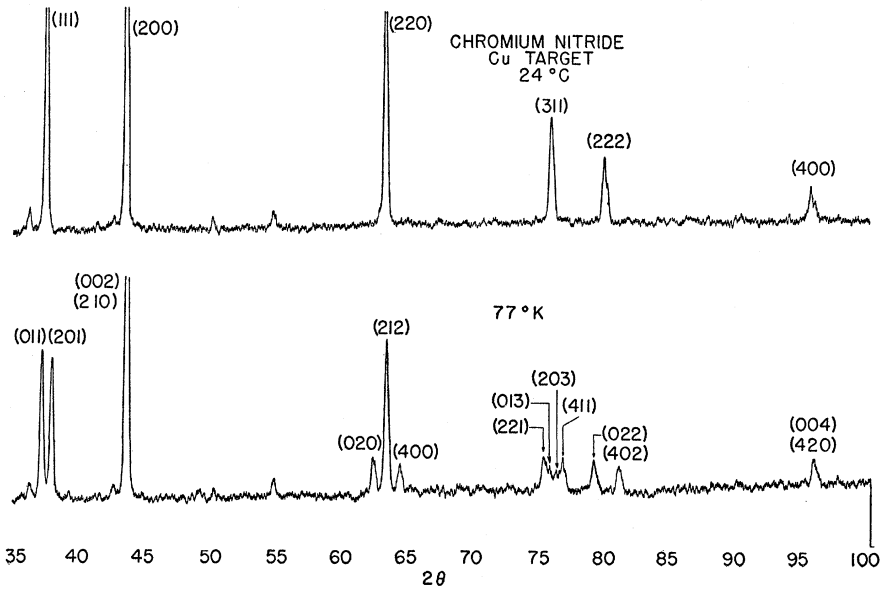

FIG. 4. X-ray diffraction traces of CrN taken at room temperature and at 77°K. The room temperature pattern is indexed on the cubic cell. The low-temperature pattern is indexed on the orthorhombic cell of Fig. 5.

TABLE III. Comparison of calculated and observed x-ray line positions in orthorhombic phase (77°K); $a=5.757$, $b=2.964$, $c=4.134$.

(*hkl*) Cubic indexing	(*hkl*) Orthorhombic indexing	2θ (calc)	2θ (obs)	(*hkl*) Cubic indexing	(*hkl*) Orthorhombic indexing	2θ (calc)	2θ (obs)
111	011 (4)[a]	37.22	37.23	222	022 (4)	79.32	79.33
	201 (4)	37.98	37.99		402 (4)	81.20	81.23
200	002 (2)	43.66	43.68	400	004 (2)	96.10	96.18
	210 (4)	43.70			420 (4)	96.22	
220	020 (2)	62.48 ↔	62.48	331	031 (4)	106.22	106.2
	212 (8)	63.59 ↔	63.59		223 (8)	107.62	107.62
	400 (2)	64.56 ↔	64.56		413 (8)	109.10	109.08
					601 (4)	110.66	110.65
311	221 (8)	75.50	75.45	420	230 (4)	110.66	
	013 (4)	75.92	75.8		214 (8)	112.54	112.57
	203 (4)	76.40	76.3		422 (8)	112.64	
	411 (8)	76.94	76.88		610 (4)	114.72	114.75

[a] Multiplicity.

discussed in some detail in a recent publication.[6] For purposes of the present discussion, it may be well to review some of the transformation properties of magnetic moments in relation to space group operations.

We may regard a space group as a collection of rotational and translational operators, which when applied to a crystal structure either singly or in combination, bring the structure into coincidence with itself. The presence of magnetic moments requires that operations of symmetry leave not only atomic positions invariant, but spin orientations as well. Symmetry operations of the first kind (translation, rotation) transform magnetic moments in the same way as the vectors conventionally associated with the moment direction; operations of the second kind (inversion, reflection) reverse the sense of the vector. In addition, magnetic structures admit the operation of reversal of spin direction, which in combination with the ordinary symmetry operations, gives rise to a complete set of antisymmetry operations (antitranslation, antirotation). An operation of antisymmetry consists of an ordinary symmetry operation followed by a reversal of the sense of the magnetic vector. Thus, in a substance containing aligned magnetic moments, a magnetic atom can be placed on any ordinary rotation axis, provided its spin is directed along the axis; and on an antirotation axis only if it is two-fold, in which case the spin must be perpendicular to the axis. A magnetic atom situated on a mirror plane must have its spin directed perpendicular to the plane, whereas the spin must lie in the plane in the case of an antimirror. Screw axes and glide planes are, of course, not subject to such restrictions.

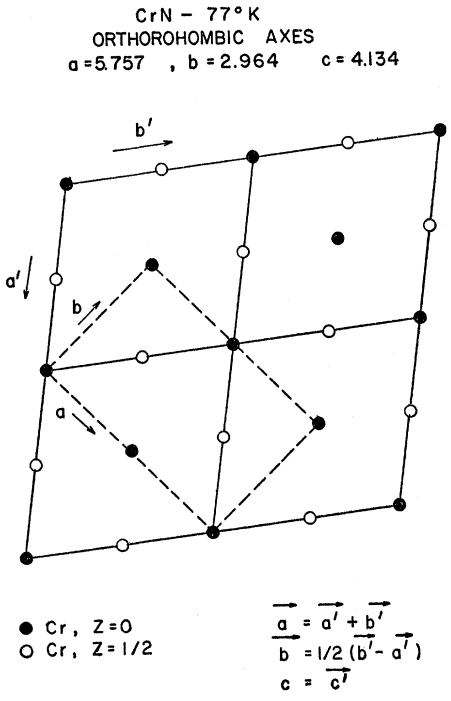

FIG. 5. Orthorhombic unit cell and relationship of orthorhombic to cubic axes.

The introduction of antisymmetry leads to an increase in the number of possible space groups from the 230 classical groups to the 1651 Shubnikov groups. The latter are simply related to the classical groups and have been derived by Belov[7] and co-workers by a

TABLE IV. Comparison of calculated line positions of the two magnetic structures of the fourth kind with observed positions.

Magnetic reflection			Peak position		
	Orthorhombic indexing		2θ (calc)		2θ (obs)
Pseudocubic indexing	(*a*) (Final model)	(*b*)	(*a*) (Final model)	(*b*)	
110	100	100	10.60	10.60	10.6
		010		10.30	
112	101	101	18.24	18.24	18.3
		011		18.06	
130	110	120	23.30	23.30	23.3
		210		23.70	

[6] G. Donnay, L. M. Corliss, J. H. D. Donnay, N. Elliott, and J. Hastings, Phys. Rev. 112, 1917 (1958).

[7] N. V. Belov, N. N. Neronova, and T. S. Smirnova, Kristallografiya 2, 315 (1957).

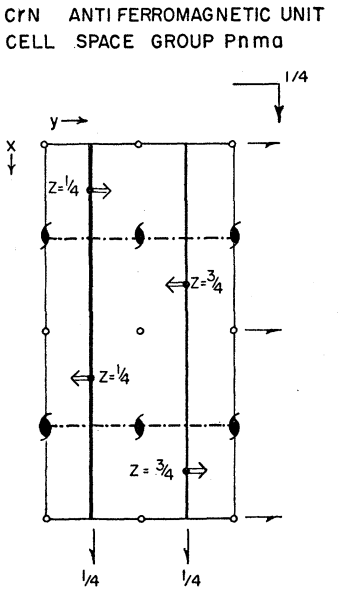

FIG. 6. Orthorhombic unit cell of CrN showing magnetic moments in relation to symmetry elements of space group *Pnma*. Symbols for symmetry elements are those of the *International Tables for X-ray Crystallography*.

systematic replacement of symmetry elements by their corresponding antisymmetry elements. For this reason, all the essential information concerning available atomic positions can be obtained from standard tabulations of the 230 classical groups.

In the case of CrN, since single crystals were not available, the usual systematic procedures for space group determination could not be followed. Nevertheless, in the present instance, it is possible to determine the allowed space group of maximum symmetry. Furthermore, to an order of accuracy consistent with our experimental uncertainty, one can show that the conclusions reached using this space group are unaltered in going to an allowed space group of lower orthorhombic symmetry.

Powder data provide the following criteria for the choice of space group: (1) the symmetry must be orthorhombic, or lower; (2) atomic positions must be close to those corresponding to the NaCl structure; and (3) the magnetic ordering scheme (ordering of the fourth kind) must be invariant under the space group operations. The last of these requirements is quite restrictive inasmuch as sets of otherwise indistinguishable positions for the metals give rise to different spin arrangements in different space groups.

Examination of the orthorhombic space groups reveals that the most symmetrical space group satisfying the above criteria is *Pnma*.[8] Both the chromium and the nitrogen atoms are placed in positions 4 (*c*):

$$x, \tfrac{1}{4}, z;\quad \bar{x}, \tfrac{3}{4}, \bar{z};\quad \tfrac{1}{2}-x, \tfrac{3}{4}, \tfrac{1}{2}+z;\quad \tfrac{1}{2}+x, \tfrac{1}{4}, \tfrac{1}{2}-z,$$

with $x\sim\frac{1}{8}$, $z\sim\frac{1}{4}$ for chromium and $x\sim\frac{1}{8}$, $z\sim\frac{3}{4}$ for nitrogen. The magnetic unit cell, together with the symmetry operators for space group *Pnma* are shown in Fig. 6. Since the metal atoms lie on mirror planes, their magnetic moments must be directed along the normals to these planes; that is, along the y axis, which, in turn, corresponds to that face-diagonal of the original cube which is elongated by the distortion. It is thus seen that the spin axis bears a simple geometric relationship to the distortion.

CALCULATIONS

If we assume that atomic displacements are small, as indicated by the approximate agreement obtained with the cubic model, the structure factors can be expanded in terms of the deviation of the positional parameters from the values $x_{Cr}=\frac{1}{8}$, $z_{Cr}=\frac{1}{4}$, $x_N=\frac{1}{8}$, $z_N=\frac{3}{4}$. Retaining only first order terms, the magnetic structure factors exhibit a dependence only on Δx, the shift in Cr position parallel to the x axis. Both the exact and approximate magnetic structure factors are listed in Table V. Excellent agreement between calculated and observed magnetic intensities can be obtained using a parameter value of $4\pi\Delta x=0.16$, corresponding to a shift of 0.073 A. This agreement is achieved without arbitrary adjustment of either the form factor or the spin direction; the latter is fixed by symmetry and the former is the Mn^{+2} experimental form factor, which should be very close to that of chromium and which has been found to work for several other chromium compounds. The magnitude of the chromium moment is obtained by internal normalization of the magnetic intensities with respect to the nuclear intensities and is found to be $2.36\mu_\beta$. A summary of the final intensity calculations is given in Table VI.

A salient feature of the neutron patterns is the appearance below the Néel point of the nuclear (211) reflection. This observation, taken together with the fact that the (202) reflection is absent, makes it possible to evaluate the shift in the nitrogen positions along the x axis. The first order structure factors for these reflections are:

$$F_{211}=16\pi(b_{Cr}\Delta x_{Cr}-b_N\Delta x_N),$$
$$F_{202}=16\pi(b_{Cr}\Delta x_{Cr}+b_N\Delta x_N).$$

TABLE V. Magnetic structure factors (F^2/p_{Cr}^2).[a]

hkl (orthorhombic indexing)	Exact	1st order approx	Zeroth order approx
100	$16\cos^2 2\pi x$	$8(1-4\pi\Delta x)$	8
101	$16\sin^2 2\pi x \sin^2 2\pi z$	$8(1+4\pi\Delta x)$	8
110	$16\sin^2 2\pi x$	$8(1+4\pi\Delta x)$	8
111	$16\cos^2 2\pi x \sin^2 2\pi z$	$8(1-4\pi\Delta x)$	8
102	$16\cos^2 2\pi x \cos^2 4\pi z$	$8(1-4\pi\Delta x)$	8
300	$16\cos^2 6\pi x$	$8(1+12\pi\Delta x)$	8

[a] p_{Cr} is the magnetic scattering amplitude of chromium.

[8] *International Tables for X-Ray Crystallography* (Kynoch Press, Birmingham, 1952), Vol. I.

The presence of (211) and absence of (202) indicate that Δx_N is opposite in sign to Δx_{Cr} and comparable in size. Comparison with the $(200)_{cubic}$ reflection, utilizing $4\pi\Delta x_{Cr}=0.16$, gives $4\pi\Delta x_N=-0.13$.

It is apparent that the foregoing analysis does not permit an evaluation of either Δz_{Cr} or Δz_N. From a qualitative analysis of the relative intensities of the split components of x-ray reflections at 77°K, one may estimate that Δz_{Cr} and Δz_N are small and probably not larger in magnitude than Δx. These variations in the z parameters can cause small nuclear contributions to some of the magnetic peaks. However, more exact calculations show that these contributions are compensated by small decreases in the magnetic intensities, leaving the net calculated intensities essentially unaltered.

The space group *Pnma*, while the most symmetrical of the space groups consistent with the data, is by no means the only possible choice. The orthorhombic space groups *Pna*2, *Pmn*2, *Pmc*2, and $P2_12_12_1$ are also satisfactory. However, in the approximation of small displacements from the atomic positions in the cubic phase, the magnetic structure factors in these space groups all reduce to the expressions obtained for *Pnma*. The physical picture would thus appear to be relatively insensitive to the choice of space group, the precise determination of which must await single crystal studies.

DISCUSSION

The final magnetic model has been shown to consist, in cubic description, of alternating double sheets parallel to a [110] direction. In terms of the orthorhombic cell of Fig. 6, these sheets lie parallel to the *yz* plane. The motion of the metal atoms, as determined by the space group parameter, x_{Cr}, results in the movement of these sheets parallel to their normal. The separation of like planes is increased by approximately ten percent while that of unlike planes is decreased in the same amount. These displacements are shown schematically by the arrows in Fig. 7. The motion of the nitrogen is given by the dashed arrow in the figure and is seen to be parallel and approximately equal in magnitude to that of the metal atoms in the $z=\frac{1}{4}$ level. Above the Néel point, each nitrogen is surrounded by a regular octahedron of chromium neighbors. The distortions, which occur in the antiferromagnetic range, tend to preserve the square arrangement in the plane of the octahedron and to destroy the symmetry along the axis at right angles to this plane. The nitrogen remains nearly symmetrically located with respect to the two pairs of antiferromagnetically coupled chromium atoms.

TABLE VI. Comparison of calculated and observed magnetic intensities.

hkl (orthorhombic indexing)	I_{calc}[a]	I_{obs}
100	833	838
101	563	560
110	54	60
111	86	86
102	55 } 101	95
300	46 }	

[a] Computed using Mn^{+2} form factor, spin parallel to *b*-axis, $\mu_{Cr}=2.36\mu_B$, $4\pi\Delta x=0.16$.

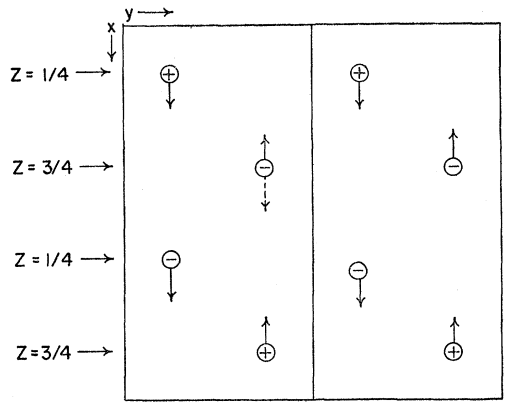

FIG. 7. Atomic displacements in CrN. Plus and minus signs refer to magnetic moments (directed parallel to the *y* axis). The solid arrows indicate the motion of the Cr atoms; the dashed arrow indicates the displacement of the nitrogen atom at the $z=\frac{1}{4}$ level.

Rundle[5] has recently given a new interpretation of the bonding in interstitial carbides, nitrides, and some oxides, having the composition *MX*. He points out that these compounds tend to have the NaCl structure regardless of the structure of the corresponding metal and its crystallographic radius, and that furthermore, strong directional metal to nonmetal bonds are required to explain their structure, hardness, brittleness, high melting-points, and conductivity. The interstitial phases are regarded as electron-deficient structures in which the nonmetal forms more bonds than it has bond orbitals. Rundle proposes that the nonmetal utilizes two hybrid *sp* orbitals and two *p* orbitals to form six bonds, two of which would be ordinary covalent bonds. Full octahedral symmetry is then achieved by resonance. In more ionic compounds it is expected that three sets of *p* orbitals are utilized by the anion to form six equivalent bonds.

In the case of the MnO-type of magnetic structure, three pairs of metal atoms are coupled antiferromagnetically through the nonmetal, utilizing, presumably, the three orthogonal *p* orbitals. In CrN one finds antiferromagnetic coupling in two of these directions and ferromagnetic coupling in the third. Using Rundle's model of the bonding, one might tentatively associate the two kinds of coupling with the *p* and *sp* orbitals, respectively. One would have to assume, in this connection, that the postulated resonance either ceases or becomes anisotropic below the Néel point.

ACKNOWLEDGMENT

We wish to thank Professor J. D. H. Donnay of the Johns Hopkins University and Dr. G. Donnay of the Carnegie Institution for helpful discussions.